



ELECTRONIC AND OPTICAL PROPERTIES OF Bi_2Se_3 TOPOLOGICAL INSULATOR: A PROMISING ABSORBING LAYER FOR BROADBAND PHOTODETECTOR

Abdullahi Lawal^{1,2}, A. Shaari¹, R. Ahmed¹, M. H Ali³ and Norshila Jarkoni¹

¹Department of Physics, Faculty of Science, Universiti Teknologi Malaysia, Skudai, Johor, Malaysia

²Department of Physics, Federal College of Education Zaria, Nigeria

³Department of Physics, Faculty of Science, Bayero University Kano, Nigeria

E-Mail: abdullahikubau@yahoo.com

ABSTRACT

Bismuth selenide (Bi_2Se_3) is a van der Waals compound which has been excellently reported as thermoelectric material. Linear dispersion near Fermi energy level is an exciting feature to consider, a promising candidate for photonic device within broadband wavelengths. For this application, detailed knowledge of its structural, electronic and optical properties is very essential. The electronic properties were determined by density functional theory (DFT) calculations implemented in Quantum-Espresso simulation package which uses plane wave basis and pseudopotential for the core electrons. Optical properties are computed by solving Bethe-Salpeter equation of many-body perturbation theory (MBPT) as implemented in Yambo code. The band structure results show the semiconducting behaviour of Bi_2Se_3 . Taken into account the effects of electron-hole interaction by solving Bethe-Salpeter equation, the calculated optical properties are in better agreement with available experimental results. The exciton energy shows that the title material can absorb light within infrared region.

Keywords: DFT, Bi_2Se_3 , BSE.

1. INTRODUCTION

Topological insulators (TIs) are new class of narrow band gap semiconducting materials characterized by the presence of strong spin orbit (SO) interactions, which invert the orbital character of conduction and valence bands [1-5]. TIs mainly Bi_2Te_3 and Bi_2Se_3 compound are narrow band gap semiconductor materials having linear dispersion with respect to the surface momentum \mathbf{k} , which are exciting features for detecting light within broadband wavelengths. The spin polarization varies with \mathbf{k} which is different from any other 2D surface states because of combination of time-reversal symmetry and spin-orbit coupling [6]. Recently, Bi_2Te_3 and Bi_2Se_3 TIs have become a hot area of study in material science because they have single Dirac cone leading to tuneable surface band gap which is a key requirement for many optoelectronic devices [7]. The main device applications of TIs based materials are optical recording, quantum computing, thermoelectric, laser photonics, broadband photo detectors and high speed optoelectronics, because of their fantastic electronic and optical properties [2, 7, 8]. Nowadays, the research on Bi_2Se_3 is in progress and researchers focused mainly on photo detectors near infrared wavelengths due to their versatile application in medicine, telecommunication, medical imaging and gas sensing [9]. Therefore, it is essential to determine bismuth selenide electronic and optical properties for better understanding of optoelectronic properties such as train edge of reflection, photocurrent sensitivity and light absorption [10, 11]. Bi_2Se_3 has rhombohedral crystal structure of five atoms per unit cell with three Te (Se) atoms differentiated by two atoms as Se-1 and the other as Se-2 which belong to (R-3m) space group while the Bi atoms are equivalent. Alternatively three rhombohedra

unit cells of Bi_2Se_3 and Bi_2Te_3 structure form hexagonal unit cell containing 15 atoms regards as quintuple layered inform of a slab of five atomic layers shown in Figure-1b [12-14]. Quintuple layers held together by van der Waals interactions along vertical axis [1, 13]. Theoretical investigation by various ab-initio methods and experimental studies has shown that Bi_2Se_3 Tis is a semiconductor material with small band gap and the gap depends strongly on spin orbit interaction [13]. Though, density functional theory (DFT) methods underestimated band gap but are practical for computation of realistic surfaces based on LDA or GGA [11].

Optical properties are used to characterize the optoelectronic behaviour of any condensed-matter systems for technical application. Therefore, it is essential to be able to accurately describe such quantities with reliable approach that provides a satisfactory description in agreement with experimental findings. Optical properties of Bi_2Se_3 have been extensively studied experimentally [15-19], compared to theoretical study. For quite decades, optical properties of the materials have been investigated extensively with standard DFT using independent particle approach of Ehenreich and Cohen [20, 21] and one-particle Green's function approach within GW approximation [22]. However, neither of these methods provides a correct evaluation of optical spectra, because the optical spectrum and the shape of the calculated dielectric function show significant differences from those obtained in experimental measurement [23-26]. The limitation of standard DFT and one-particle Green's function is their failure to describe the excitonic effect of electron-hole interaction which requires two-particle approach. Therefore, for effective description of optical spectra, the excitonic effect due to electron-hole interaction



should be included. Moreover, to the best of our knowledge, *ab initio* calculations of optical properties with the inclusion of electron-hole effects for Bi₂Se₃ have not been reported yet.

In this paper, electronic properties of Bi₂Se₃ in hexagonal structure are calculated using first-principles approach within DFT framework. For optical properties, we employed a technique that introduced electron-hole interaction into first-principles many-body perturbation theory (MBPT) via Bethe-Salpeter equation (BSE) approach as implemented in YAMBO package.

2. THEORETICAL METHODOLOGY

The electronic structures of Bi₂Se₃ in hexagonal structure were calculated by pseudopotential method within density functional theory (DFT) using plane-wave as a basis set. The electron-electron interactions were treated with generalized gradient approximation (GGA) in the form of Perdew-Berke-Ernzndof (PBE) functional. Full relativistic pseudopotentials were used throughout. The SOC is included in the calculation as Bi and Se atoms are heavy elements, the effects were treated using fully relativistic norm-conserving pseudopotentials. The calculations were performed within the Quantum-Espresso package[27]. Plane-wave kinetic energy cutoffs were set at 82 Ry with charge density of 475 Ry for the bulk and the surface respectively. The Brillouin zone was sampled with a 10×10×10 Monkhorst-Pack grid of k-points. The geometry relaxation calculations were performed as a results of the Born Openheimer approximation, this stage involves the determination of the cell parameters and the atomic coordinates that minimize the energy function within the adopted numerical approximations using the Broyden-Fletcher-Goldfarb-Shanno (BFGS) algorithm[27, 28]. Optical properties were calculated via solving MBPT as implemented in Yambo code[29]. The calculation of dielectric function $\epsilon(w)$ is on 8×8×10 Monkhorst-Pack mesh and 30 eV are taken to build up BSE kernel for electron-hole while 0.1 eV damping coefficient were used for the static dielectric matrices.

The imaginary part of dielectric function $\epsilon_2(\omega)$ was obtained by direct electronic transitions between occupied and unoccupied electronic states and calculated from Eq.1 [24], while Kramers-Kronig relations was used for calculating real part of frequency dependent dielectric function as shown in Eq.2 [30].

$$\epsilon_2(\omega) = \frac{16\pi e^2}{\omega^2} \sum_s |\vec{\lambda} \cdot \langle O | \vec{v} | S \rangle|^2 \delta(\omega - \Omega^s) \quad (1)$$

$$\epsilon_1(\omega) = 1 + \frac{2P}{\pi} \int_0^\infty \frac{\omega' \epsilon_2(\omega')}{\omega'^2 - \omega^2} d\omega' \quad (2)$$

where $\vec{\lambda}$ is the polarization vector of light. $\langle O | \vec{v} | S \rangle$ is the optical transition matrix from valence to conduction states and P is the principal value of the integral and the integral is over irreducible Brillouin zone.

3. RESULTS AND DISCUSSIONS

3.1 Structural properties

The optimized lattice constants are shown in Table-1. We found that estimated c is the largest source of errors for every xc functional because the bonding in z direction is van der Waals force. Table-1 presents the fully relaxed lattice parameters and internal atomic coordinates of Bi₂Se₃ in hexagonal structure along with experimental and previous *ab initio* results. From our first principles calculation, we observed that GGA (PBE) tend to overestimate lattice parameter c and interlayer distance d_{eqm} . Interestingly, we noticed that a , c , d_{eqm} as well as internal atomic coordinates μ for Bi and ν for Se atoms, with the inclusion of vdW corrections are in good agreement with experimental results. Therefore, our first-principles calculation suggest that vdW correction is important for predicting lattice parameters and interlayer distance in the case of Bi₂Se₃, as it gives best matching with experimental results.

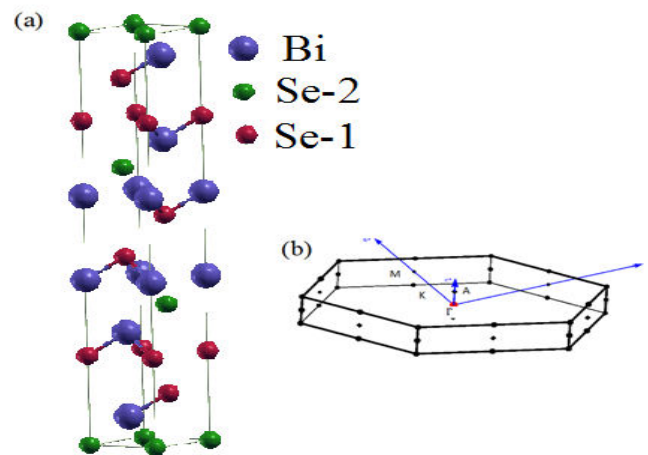


Figure-1. Structure of Bi₂Se₃ (a) Bulk Hexagonal unit cell. (b) First Brillouinzone along the high symmetry points.



Table-1. Calculated lattice parameter of Bi₂Se₃ compared with previous theoretical and experimental.

Structure	Work	Method	Lattice parameters	
			a(Å)	c(Å)
Hexagonal unit cell	Our work	PBE	4.183	31.336
		PBE+vdW	4.134	28.758
	Previous work	LDA[31]	4.140	27.610
		PBE+SOC [6]	4.195	31.010
		PBE [6]	4.178	31.860
		Exp.[32]	4.143	28.630

3.2 Electronic properties

The band structures calculation of Bi₂Se₃ within GGA with taking into account the spin-orbit coupling along high-symmetry points $\Gamma \rightarrow M \rightarrow K \rightarrow \Gamma \rightarrow A$, $\Gamma(0.0000 \ 0.0000 \ 0.0000)$, $M(0.3333 \ 0.0000 \ 0.0000)$, $K(0.5000 \ 0.0000 \ 0.0000)$ and $A(0.0000 \ 0.0000 \ 0.5000)$ of the first Brillouin zone are plotted by setting Fermi energy level to be 0 eV on energy scale in band structure and density of states plots as shown in Figures 2 and 3. The band structures and total density of states calculations show that the bottom of the conduction band and the top of valence band occurred at the Γ point indicating a direct band gap of value around 0.14 eV. This value is smaller than experimental band gap of 0.32-0.35 eV [19, 33, 34]. Underestimation of band gap is the limitation of DFT approach due to approximations used for the exchange-correlation functional. The results of total and partial densities of states (DOS and PDOS) helps to further elaborate the nature of band gap as shown in Figures 3 and 4. The partial density of states gives information about the origin of bands. The s-orbital of Bi and the s-orbital of both Se-1 and Se-2 atoms contribute the most states to the core bands while p-orbitals of Se-1 and Se-2 contribute the most states to valence bands. The p-orbitals of Bi atoms contribute the most to the conduction bands.

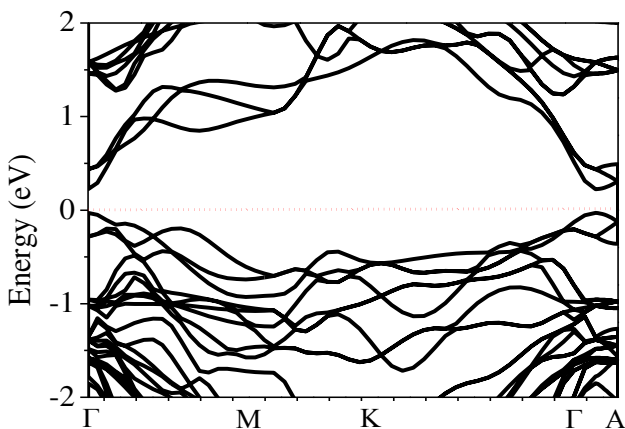


Figure-2. Band structure of bulk Bi₂Se₃ with SOC.

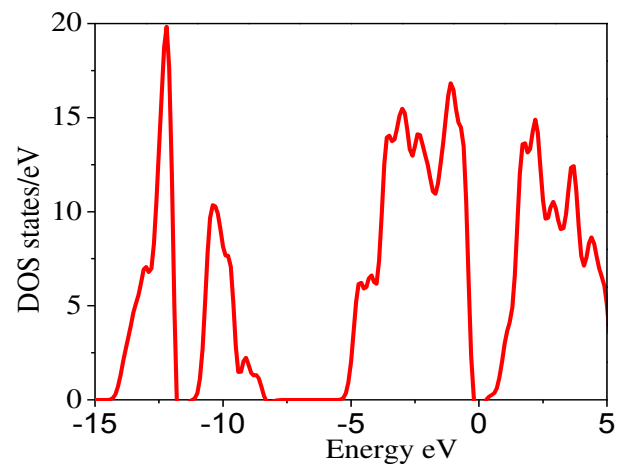


Figure-3. Total density of state DOS for Bi₂Se₃.

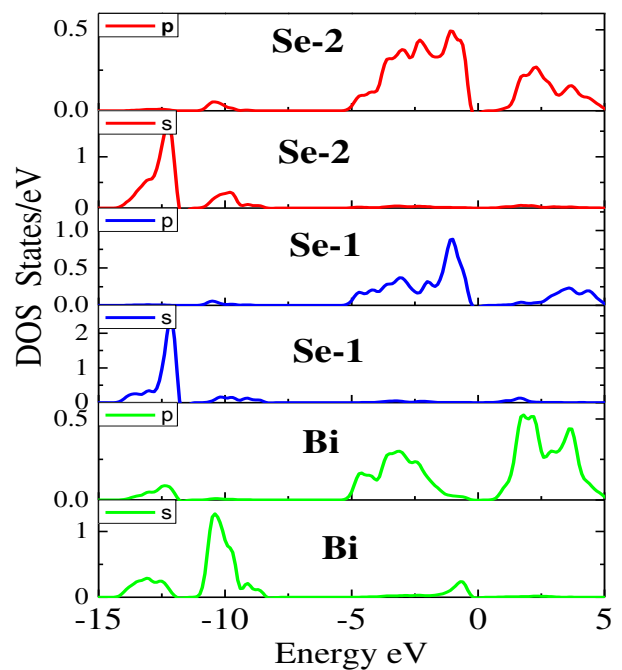


Figure-4. Partial density of state for Bi₂Se₃.



3.3 Optical properties

Optical properties investigation of materials plays a role in understanding their optoelectronic application. We have calculated the optical properties by evaluating microscopic dielectric function $\epsilon(\omega)$ via two different approaches: Random phase approximation (RPA) based on PBE (DFT+RPA) without taking into account the electron-electron and electron-hole interaction and solving BSE of many-body perturbation theory (MBPT) based on two interacting QP scheme on top of DFT results to include the role of interaction between the excited electron and hole left in the valence band region BSE methods were used for optical properties via solving MBPT as implemented in Yambo code [35]. Although, the investigation of material optical properties with BSE is computationally expensive but provides an accurate description of the experimental absorption spectra. Real and imaginary parts of dielectric function were calculated with polarization along z-direction direction. The electronic at high frequency and ionic contributions of a non-polar system is contained in the static dielectric permittivity tensor $\epsilon(0)$. The dielectric constant $\epsilon(\infty)$ at high frequency obtained to be 16.3 and 29.3 for DFT+RPA and BSE respectively, showing that the dielectric constant at high frequency obtained via BSE is in good agreement with experimental value of 29.0 [17, 18, 36]. The first edge of the imaginary part of the dielectric function in the case of DFT+RPA, called optical absorption edge is due to the inter-band transition between conduction band minimum and valence band maximum states was found to be 0.15 eV and this value is correspond to the fundamental band gap of the material. The description of optical properties with excitonic effects of electron-hole interaction via BSE gives indeed a definite improvement of results over DFT+RPA as can be seen in Table-2. Comparing the location of fundamental gap edge within DFT+RPA and the shifted excitonic peak due to BSE, we deduced an exciton binding energy of 0.21 eV. The exciton energy reveals that Bi_2Se_3 compound can absorb light in the infrared region. Occurrence of highest peak at 1.9 eV by BSE indicated that the title material has strong absorption and low electron losses at lower energy. The change of real part of dielectric function from positive to negative at 1.6 eV suggests that the Plasmons of Bi_2Te_3 material should resonate at energy greater than 1.6 eV. Thus, for the plasmonic behaviour, after which $\epsilon_1(\omega)$ becomes negative, we observed a steep decrease between 1.6 to 2.5 eV and eventually increases slowly toward zero (epsilon-near-zero) above 5 eV in the UV region. This epsilon-near-zero behaviour of Bi_2Te_3 is another exciting feature for many applications [37-39]. The relatively strong absorption in 0.34s-16.3 eV energy range provides strong evidence that Bi_2Se_3 TI has the potential to be used for detecting light within broadband range.

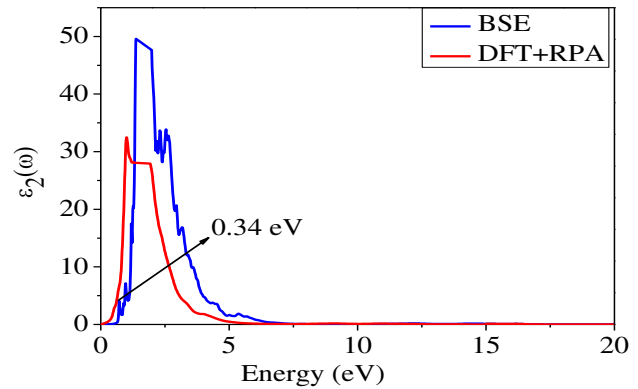


Figure-5. Imaginary part of the dielectric function of Bi_2Se_3 calculated using DFT+RPA and G_0W_0 +BSE.

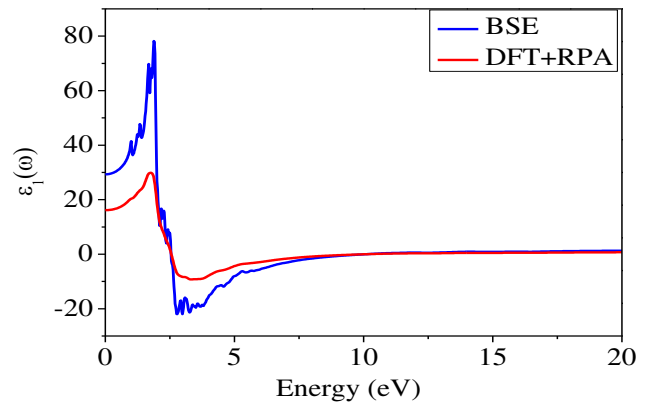


Figure-6. Real part of the dielectric function of Bi_2Se_3 calculated using DFT+RPA and G_0W_0 +BSE.

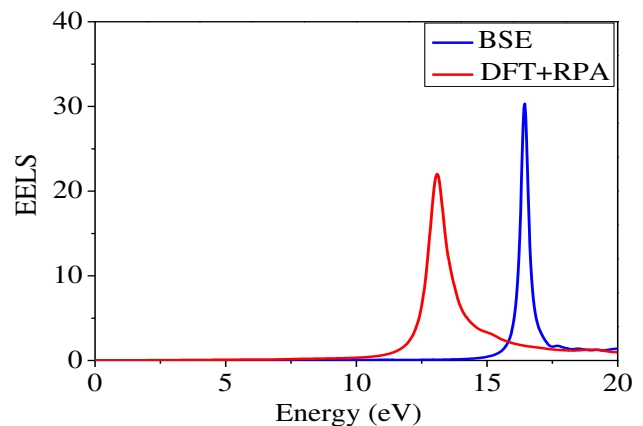


Figure-7. EELS calculated using DFT+RPA and G_0W_0 +BSE.

**Table-2.** Bi₂Se₃DFT+RPA and BSE results compared with experimental data.

		Optical gap (eV)	$\epsilon(\infty)$	Plasma energy (eV)
Our work	DFT+RPA	0.14	23.1	19.3
	BSE	0.34	29.3	16.4
Previous	Experimental	0.3[40], 0.32 [19]	29.0[18], 29.0 [36]	16.8[41], 16.5 [42]

The spectrum shape and values of the maximum peak via BSE are in quite good agreement with experimental results [43, 44], due to the exact description of electron-hole exchange and excitonic effects in solution of MBPT. Figure-7 is a graph of electron energy loss function, which is a tool that describes the loss in energy of a fast moving electron in a material from top of a valence band to bottom of a conduction band. The feature behavior of the prominent peaks in the spectra represents the characteristics of plasma resonance. Such peaks describe the train edge of reflection spectra. At this point of energy the real part of the dielectric function goes to zero indicating strong reflection of light in the ultra violet region due to small electron loss. The prominent peak was found to be 16.3 eV for BSE and this value is consistent with experimental data [42].

4. CONCLUSIONS

In this paper, structural and electronic properties of Bi₂Se₃ topological insulator were investigated using *ab initio* pseudopotential approach within DFT implemented in the Quantum Espresso package. The calculated result shows that Bi₂Se₃ is a narrow gap semiconductor material. The calculated optical properties after adding electron-hole interactions (BSE) are in good agreement with experimental results. Our theoretical approach highlighted the effectiveness of including electron-hole corrections for accurate theoretical prediction of optical properties of Bi₂Se₃ and other similar compounds like Bi₂Te₃, Sb₂Te₃ and Sb₂Se₃.

ACKNOWLEDGEMENTS

The authors acknowledge FRGS research grant (Vot No.4F915) from ministry of High Education Malaysia, Universiti Teknologi Malaysia (UTM), TETFund through Federal College of Education Zaria, Kaduna, Nigeria and Center for information and Communication Technology (CICT) in University Teknologi Malaysia for financial support, facilities and services of high performance computing on this research work.

REFERENCES

[1] Hasan M.Z. and C.L. Kane. 2010. Colloquium: topological insulators. *Reviews of Modern Physics*. 82(4): 3045.
[2] Wang Z., *et al.* 2016. Harmonic mode-locking and wavelength-tunable Q-switching operation in the

grapheme-Bi₂Te₃ heterostructure saturable absorber-based fiber laser. *Optical Engineering*. 55(8): 081314-081314.

[3] Yazyev O.V., J.E. Moore and S.G. Louie. 2010. Spin polarization and transport of surface states in the topological insulators Bi₂Se₃ and Bi₂Te₃ from first principles. *Physical review letters*. 105(26): 266806.
[4] Kaczkowski J. and A. Jezierski. 2008. First-principles study of X/Bi₂Te₃ (0001) surface (X= Ag, Ni, Ti). *Materials Science Poland*. 26(4): 939--845.
[5] Lawal A., *et al.* 2017. First-principles many-body comparative study of Bi₂Se₃ crystal: A promising candidate for broadband photodetector. *Physics Letters A*. 381(35): 2993-2999
[6] Luo X., M.B. Sullivan and S.Y. Quek. 2012. First-principles investigations of the atomic, electronic, and thermoelectric properties of equilibrium and strained Bi₂Se₃ and Bi₂Te₃ including van der Waals interactions. *Physical Review B*. 86(18): 184111.
[7] Moore J.E. 2010. The birth of topological insulators. *Nature*. 464(7286): 194-198.
[8] Sharma A., *et al.* 2016. High performance broadband photo detector using fabricated nanowires of bismuth selenide. *Scientific reports*. 6.
[9] Zhu H., *et al.* 2013. Topological insulator Bi₂Se₃ nanowire high performance field-effect transistors. *Scientific reports*. 3.
[10] Sun L., *et al.* 2014. Preparation of few-layer bismuth selenide by liquid-phase-exfoliation and its optical absorption properties. *Scientific reports*. 4: 4794.
[11] Gao X., *et al.* 2016. First-principles study of structural, elastic, electronic and thermodynamic properties of topological insulator Bi₂Se₃ under pressure. *Philosophical Magazine*. 96(2): 208-222.



- [12] Crowley J.M., J. Tahir-Kheli, and W.A. Goddard III. 2015. Accurate Ab Initio Quantum Mechanics Simulations of Bi₂Se₃ and Bi₂Te₃ Topological Insulator Surfaces. *The Journal of Physical Chemistry Letters*. 6(19): 3792-3796.
- [13] Lawal A., *et al.* 2017. Sb₂Te₃ crystal a potential absorber material for broadband photodetector: A first-principles study. *Results in Physics*. 7: 2302-2310.
- [14] Zhang W., *et al.* 2010. First-principles studies of the three-dimensional strong topological insulators Bi₂Te₃, Bi₂Se₃ and Sb₂Te₃. *New Journal of Physics*. 12(6): 065013.
- [15] Gobrecht H., S. Seeck and T. Klose. 1966. Der Einfluß der freien Ladungsträger auf die optischen Konstanten des Bi₂Se₃ im Wellenlängengebiet von 2 bis 23 µm. *Zeitschrift für Physik*. 190(4): 427-443.
- [16] Nataraj D., *et al.* 1999. Effect of annealing on optical, dielectric and ac conduction properties of Bi₂Se₃ thin films.
- [17] Humlíček J., *et al.* 2014. Raman and interband optical spectra of epitaxial layers of the topological insulators Bi₂Te₃ and Bi₂Se₃ on BaF₂ substrates. *Physica Scripta*. 2014(T162): 014007.
- [18] Kalampokis A., E. Hatzikraniotis and K. Paraskevopoulos. 1998. Study of the deintercalation process in Bi₂Se₃ single crystals treated with hydrazine. *Materials research bulletin*. 33(9): 1359-1366.
- [19] Larson P., *et al.* 2002. Electronic structure of Bi₂X₃ (X= S, Se, Te) compounds: Comparison of theoretical calculations with photoemission studies. *Physical review B*. 65(8): 085108.
- [20] Hedin L., S. 1969. *Lundqvist in Solid State Physics* edited by Seitz, F., Turnbull, D. & Ehrenreich, H. Academic Press.
- [21] Park J.-W., *et al.* 2009. Optical properties of pseudobinary GeTe, Ge₂Sb₂Te₅, GeSb₂Te₄, GeSb₄Te₇, and Sb₂Te₃ from ellipsometry and density functional theory. *Physical Review B*, 2009. 80(11): 115209.
- [22] Hedin L. 1965. New method for calculating the one-particle Green's function with application to the electron-gas problem. *Physical Review*. 139(3A): A796.
- [23] Rohlffing M., P. Krüger and J. Pollmann. 1995. Quasiparticle band structure of CdS. *Physical review letters*. 75(19): 3489.
- [24] Rohlffing M. and S.G. Louie. 2000. Electron-hole excitations and optical spectra from first principles. *Physical Review B*. 62(8): 4927.
- [25] Marsili M., *et al.* 2016. Large scale GW-BSE calculations with N₃ scaling: excitonic effects in dye sensitised solar cells. *arXiv preprint arXiv:1603.05427*.
- [26] Park J.-W., *et al.* 2008. Optical properties of (GeTe, Sb₂Te₃) pseudobinary thin films studied with spectroscopic ellipsometry. *Applied Physics Letters*. 93(2): 1914.
- [27] Giannozzi P., *et al.* 2009. Quantum Espresso: a modular and open-source software project for quantum simulations of materials. *Journal of physics: Condensed matter*. 21(39): 395502.
- [28] Stewart J.J. 1990. MOPAC manual. A general molecular orbital package. DTIC Document.
- [29] Marini A. 2016. The Yambo code: a comprehensive tool to perform ab-initio simulations of equilibrium and out-of-equilibrium properties. in *APS Meeting Abstracts*.
- [30] Lucarini V., *et al.* 2005. *Kramers-Kronig relations in optical materials research*. Vol. 110. Springer Science & Business Media.
- [31] Förster T., P. Krüger and M. Rohlffing. 2015. Ab initio studies of adatom- and vacancy-induced band bending in Bi₂Se₃. *Physical Review B*. 91(3): 035313.
- [32] Nakajima S. 1963. The crystal structure of Bi₂Te_{3-x}Se_x. *Journal of Physics and Chemistry of Solids*. 24(3): 479-485.
- [33] Smith M.J., E. Kirk and C. Spencer. 1960. Device for Measurement of the Electrical Properties of Bi₂Se₃ at Elevated Temperatures. *Journal of Applied Physics*. 31(8): 1504-1505.
- [34] Black J., *et al.* 1957. Electrical and optical properties of some M₂v- bN₃vi- b semiconductors. *Journal of Physics and Chemistry of Solids*. 2(3): 240-251.



- [35] Marini A., *et al.* 2009. Yambo: an ab initio tool for excited state calculations. *Computer Physics Communications*. 180(8): 1392-1403.
- [36] Eddrief M., F. Vidal and B. Gallas. 2016. Optical properties of Bi₂Se₃: from bulk to ultrathin films. *Journal of Physics D: Applied Physics*. 49(50): 505304.
- [37] Savoia S., *et al.* 2015. PT-symmetry-induced wave confinement and guiding in ϵ -near-zero metamaterials. *Physical Review B*. 91(11): 115114.
- [38] Li Y. and N. Engheta, Supercoupling of surface waves with ϵ -near-zero metastructures. *Physical Review B*, 2014. 90(20): 201107.
- [39] Rodríguez-Fortuño F.J., A. Vakil and N. Engheta. 2014. Electric levitation using ϵ -near-zero metamaterials. *Physical review letters*. 112(3): 033902.
- [40] Zhang J., *et al.* 2011. Raman spectroscopy of few-quintuple layer topological insulator Bi₂Se₃ nanoplatelets. *Nano letters*. 11(6): 2407-2414.
- [41] Liou S., *et al.* 2013. Plasmons dispersion and nonvertical interband transitions in single crystal Bi₂Se₃ investigated by electron energy-loss spectroscopy. *Physical Review B*. 87(8): 085126.
- [42] Nascimento V., *et al.* 1999. XPS and EELS study of the bismuth selenide. *Journal of electron spectroscopy and related phenomena*. 104(1): 99-107.
- [43] Sharma Y., *et al.* 2012. Electronic structure, optical properties and Compton profiles of Bi₂S₃ and Bi₂Se₃. *Solid State Sciences*. 14(2): 241-249.
- [44] Green A.J., *et al.* 2016. Surface oxidation of the topological insulator Bi₂Se₃. *Journal of Vacuum Science & Technology A: Vacuum, Surfaces, and Films*. 34(6): 061403.